Observations of Broadband Shear Alfven-Wave Instabilities

doi: 10.1103/PhysRevLett.47.183

Observations of Broadband Shear Alfvén-Wave Instabilities

R. Hatakeyama
Department of Electronic Engineering, Tohoku University, Sendai, Japan

and

M. Inutake[a]
Institute of Plasma Physics, Nagoya University, Nagoya, Japan

and

T. Akitsu
Department of Electronic Engineering, Kyoto University, Kyoto, Japan
(Received 1 May 1980; revised manuscript received 28 April 1981)

Shear Alfvén waves accompanied by a broad spectrum of magnetic fluctuations are observed to be destabilized by a weak field-aligned current, and resultant strong plasma diffusion is caused. The instability with frequencies much higher than an electron diamagnetic drift frequency is considered to be driven by a resistivity gradient and current in a finite-β plasma.

PACS numbers: 52.35.Bj, 52.35.Py

Microinstabilities in finite-β plasmas have attracted special interest in connection with anomalous transport of magnetically confined plasmas induced by magnetic field fluctuations,[1,2] and in magnetospheric studies.[3] Coupled drift-Alfvén waves with low frequencies have been an area of active research[4,5] in such electromagnetic instabilities. Higher-frequency Alfvén-wave instabilities driven by currents or ion beams, on the other hand, have not received as much attention despite some theoretical considerations.[6,7] In this paper, we present the first observation of shear Alfvén-wave instabilities with a turbulent spectrum in a finite-β, current-carrying, inhomogeneously resistive plasma.

A quasisteady (1 msec), current-free, highly ionized, high-density plasma (helium, $n_0 \simeq 5\times10^{14}$ cm^{-3}, $T_e \simeq T_i \simeq 5$ eV, $\beta \sim 2\%$, diameter 5 cm, length $L = 200$ cm) was produced in a uniform magnetic field ($B_{0z} \lesssim 3$ kG) by a magneto-plasma-dynamic (MPD) arcjet as shown in Fig. 1(a). The current parallel to the magnetic field was forced to flow between the plasma source and a target electrode set at one end of the device, where a positive pulse voltage was applied. Profiles of current density J_0 were obtained from the azimuthal magnetic field $B_{0\theta}$ produced in the plasma and controlled by changing the diameter of the target electrode. Experimental results for the case of a 25-mm-diam target are presented in this report. Plasma parameters were measured with a HCN interferometer, a spectrometer, double probes, and magnetic probes. The safety factor $q \equiv 2\pi r B_{0z}/LB_{0\theta}$ is larger than 5. Auto- and cross-power spectra of magnetic fluctuations were obtained by digital data processing techniques and discrete Fourier analysis.

When the current is drawn in the quiescent plasma, strong magnetic fluctuations $\omega\tilde{B}_\theta$ appear and an almost simultaneous decrease in the density is also observed as displayed in Fig. 1(b), where the target current I_T is 0.8 kA ($J_0 \simeq 80$ A/cm^2) and $B_{0z} = 2.8$ kG. From measurements of axial and radial density profiles, the radial plas-

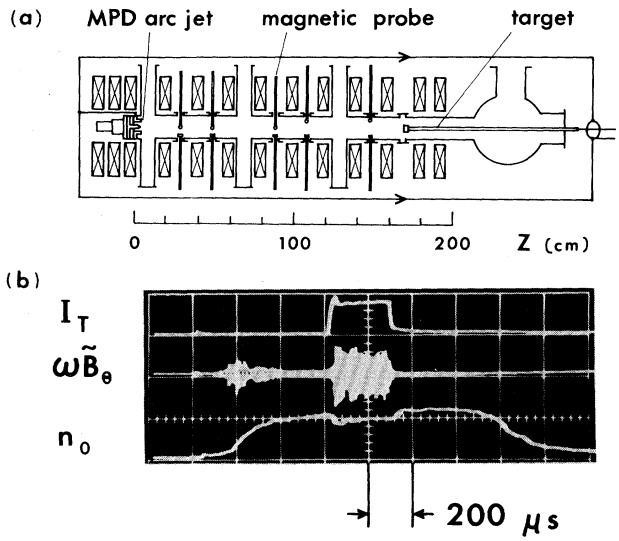

FIG. 1. (a) Experimental apparatus. Loops of return current are also shown. (b) Time evolutions of target current, azimuthal magnetic field fluctuation, and density.

ma diffusion is confirmed and considered to be due to the instability. The auto-power spectrum of $\tilde{B}_\theta$ for this case is presented in Fig. 2(a), and has dominant frequencies of 100–350 kHz, which are much higher than the density-gradient electron diamagnetic frequency $\omega_e^*/2\pi \simeq 10$ kHz and lower than the ion-cyclotron frequency $\omega_{ci}/2\pi = 1.1$ MHz. With an increase in J_0, the amplitude increases and the spectrum becomes broader, extending to the higher frequency. Dependence of the squared amplitude normalized by the axial magnetic field on J_0 is given for $\omega/2\pi = 300$ kHz in Fig. 2(b). The threshold value of an electron drift velocity v_d for driving the instability is small and on order of $0.1 v_A$ (Alfvén velocity).

Radial profiles of $\tilde{B}_{r,\theta,z}$ are shown in Fig. 3(a) as well as n_0, T_e, and J_0. The produced $B_{0\theta}$ is much smaller than B_{0z}. J_0 flows uniformly near the center of the plasma cross section ($r \lesssim 1.0$ cm), where distributions of n_0 and T_e are relatively homogeneous. The gradient of T_e is a maximum in the region $1.0 < r \lesssim 2.0$ cm, where $\tilde{B}_{\theta,z}$ have peak amplitudes. In the outer edge of the plasma ($r > 2.0$ cm) the strong gradient of J_0 and fluctuations with small amplitudes exist. Axial phase velocity of the fluctuations was determined from the cross-power phase spectrum between two signals picked up by field-aligned probes. A typical example is presented in Fig. 3(b). The phase velocity of magnetic fluctuations agrees reasonably with the local Alfvén speed calculated from B_{0z} and n_0, and they propagate axially in the direction of the current flow (i.e., opposite to the electron drift) and azimuthally in the direction of the ion diamagnetic drift with mode number $m = 1$. The same results were obtained when the direction of the external mag-

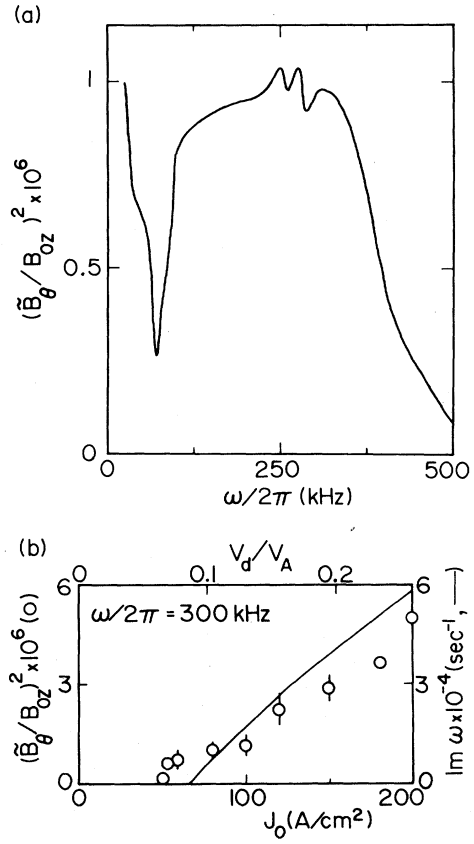

FIG. 2. (a) Power spectrum of instabilities for $J_0 \simeq 80$ A/cm^2 at $z = 105$ cm. (b) Squared amplitude of instability vs current density or normalized electron drift velocity. Solid line is the theoretical growth rate.

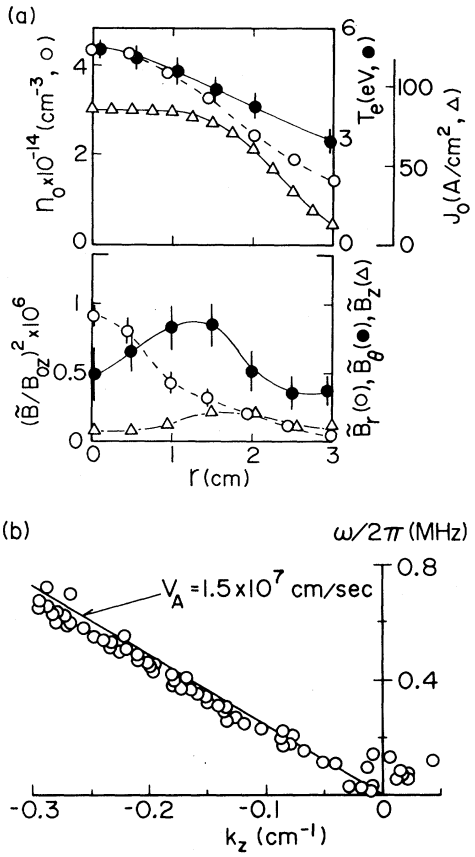

FIG. 3. (a) Radial profiles of plasma density, electron temperature, current density (upper figure), and squared amplitudes of three component magnetic fields (lower figure) for $I_T = 0.8$ kA. (b) Frequency vs axial wave number when current is directed oppositely to the axial magnetic field. Distance between the two probes is 20 cm. Solid line gives the theoretical phase velocity.

netic field was reversed. From these measurements it is concluded that the instability always has such a characteristic as $J_0 k_\theta k_z < 0$, where the signs of J_0 and k_z are chosen so as to be positive in the direction of B_{0z} (k_z and k_θ are axial and azimuthal wave numbers, respectively). The measured features mentioned above are quite different from those of drift-Alfvén waves,[5] and fluctuations with lower frequencies ($\lesssim 30$ kHz) in Fig. 2(a) were measured to be drift-Alfvén waves.

The theory considers a finite-β incompressible slab plasma with inhomogeneous resistivity $\eta_0(x)$ and uniform n_0 including a current $J_0(x)$ parallel to the z axis in a strong axial magnetic field $B_0 = \{0, B_{0y}(x), B_{0z}\}$ ($B_{0z} \gg B_{0y}$). The linearized magnetohydrodynamic equations can be written in the form

$$\rho_0 \frac{\partial \vec{v}}{\partial t} = -\nabla P + \mu_0^{-1}(\nabla \times \vec{B}) \times \vec{B}_0, \tag{1}$$

$$\frac{\partial \vec{B}}{\partial t} = (\vec{B}_0 \cdot \nabla)\vec{v} - (\vec{v} \cdot \nabla)\vec{B}_0 - \nabla \times \left(\frac{\eta_0}{\mu_0} \nabla \times \vec{B}\right) - \nabla \times (\eta \vec{J}_0), \tag{2}$$

$$\nabla \cdot \vec{v} = 0, \tag{3}$$

where η_0 of a fully ionized plasma is a function of $T_e(x)$ only. The $\vec{J}_0 \times \vec{B}$ term in Eq. (1) is negligibly small under the present parameters. Taking the perturbation to be of the form $\sim f(x) \exp(-i\omega t + ik_y y + ik_z z)$, Eqs. (1)–(3) can be combined to yield the dispersion relation for shear Alfvén waves in the case where the perturbation is nearly independent of x:

$$\left(\omega^2 - k_z^2 v_A^2 + i\omega \frac{\eta_0 k^2}{\mu_0}\right)^2 - \frac{3B_{0z}\eta_0^2 J_0 k_y k_z}{2\mu_0^2 P_0} \frac{\partial \ln \eta_0}{\partial x} \omega^2 - i \frac{B_{0y}\eta_0 J_0 k_z^2 v_A^2}{\mu_0 P_0} \frac{\partial \ln J_0}{\partial x} \omega - i \frac{3\eta_0 J_0^2 k_y^2}{2P_0 k^2} \omega^3 = 0, \tag{4}$$

where $k^2 = k_y^2 + k_z^2$, $P_0 = n_0 T_e$, and $v_A^2 = B_{0z}^2/\mu_0 \rho_0$. In the absence of current Eq. (4) gives the resistive damping of the Alfvén wave. The second term is due to the interaction between a current and a resistivity gradient, and is destabilizing when $J_0 k_y k_z \, \partial \ln \eta_0/\partial x < 0$. The third and fourth terms represent a stabilizing effect due to the current-density gradient, or magnetic shear, and a small amount of Ohmic heating, respectively. [If we had not assumed the plasma to be incompressible, then Eq. (4) would have additional terms representing the coupling, due to J_0 and η_0, between the shear Alfvén and magnetosonic modes, but these terms are negligible.] Since the last two terms are negligibly small except at the plasma edge and the measured profile of T_e gives $\partial \ln \eta_0/\partial x (\simeq 0.3 \text{ cm}^{-1}) > 0$, we obtain $\omega \simeq k_z v_A$ and $\mathrm{Im}\omega \simeq -\eta_0 k^2/2\mu_0 + [(-3B_{0z}\eta_0^2 J_0 k_y k_z/8\mu_0^2 P_0) \times \partial \ln \eta_0/\partial x]^{1/2}$ for $J_0 k_y k_z < 0$, which agrees with the measured condition, $J_0 k_\theta k_z < 0$. Calculated results are presented in Figs. 2(b) and 3(b) for $n_0 = 4 \times 10^{14} \text{ cm}^{-3}$, $B_{0z} = 2.8$ kG, and $|k_y| = 0.7 \text{ cm}^{-1}$, which are qualitatively consistent with the measured results, although the turbulent spectrum in Fig. 2(a) cannot be obtained from this linear theory. In Fig. 2(b) measured $\tilde{B}_\theta^2$ are compared with theoretical $\mathrm{Im}\omega$, since the linear growth rate should be proportional to the square of the saturation amplitude of the instability.[8] It is to be noted that the Kadomtsev theory in the low-β limit[6] does not explain our experimental results at all. Details of the theory will be published elsewhere.

Finally, when the diameter of the target is increased, the higher-frequency instabilities remain unchanged, accompanied by the dominant appearance of low-frequency current-driven drift-Alfvén waves. In conclusion, shear Alfvén waves with the broad spectrum are destabilized in the finite-β current-carrying plasma with the resistivity gradient. This work is instructive to explain magnetic fluctuations in the magnetosphere[3] and in the Macrotor tokamak,[2] and to discuss plasma transport in controlled fusion experiments.[9]

The authors express their sincere gratitude to Professor N. Sato, Professor R. Itatani, and Professor H. Ikegami for their discussions, and to Mr. S. Kishimoto for his technical assistance. This work was carried out under the collaborating research program at the Institute of Plasma Physics, Nagoya University.

[a]Present address: Plasma Research Center, University of Tsukuba, Ibaraki, Japan.

[1]W. M. Tang *et al.*, Nucl. Fusion 16, 191 (1976); A. Hasegawa *et al.*, Phys. Rev. Lett. 44, 248 (1980);

J. F. Drake *et al.*, Phys. Rev. Lett. 44, 994 (1980).
[2]S. J. Zweben *et al.*, Phys. Rev. Lett. 42, 1270 (1979).
[3]A. Nishida, *Physics and Chemistry in Space—Geomagnetic Diagnosis of the Magnetosphere* (Springer-Verlag, New York, 1978), Vol. 9, Chap. 5; N. A. Saflekos *et al.*, J. Geophys. Res. 83, 1493 (1978).
[4]K. T. Tsang *et al.*, Phys. Rev. Lett. 41, 557 (1978); Y. C. Lee and L. Chen, Phys. Rev. Lett. 42, 708 (1979); J. L. Sperling and D. K. Bhadra, Plasma Phys. 21, 225 (1979).
[5]Y. Nishida and K. Ishii, Phys. Rev. Lett. 33, 352 (1974); J. T. Tang and N. C. Luhman, Jr., Phys. Fluids 19, 1935 (1976).
[6]B. B. Kadomtsev, Zh. Tech. Fiz. 31, 1209 (1961) [Sov. Phys. Tech. Phys. 6, 882 (1962)]; L. C. Woods, Phys. Fluids 6, 729 (1963); D. A. McPherson, Phys. Fluids 9, 1373 (1966).
[7]H. L. Berk *et al.*, Nucl. Fusion 15, 819 (1975); M. N. Rosenbluth and P. H. Rutherford, Phys. Rev. Lett. 34, 1428 (1975).
[8]L. D. Landau and E. M. Lifshitz, *Fluids Mechanics* (Pergamon, London, 1960), p. 104.
[9]C. M. Surko and R. E. Slusher, Phys. Rev. Lett. 37, 1747 (1976), and Phys. Fluids 23, 2425 (1980).

Monte Carlo Calculation of Argon Clusters in Homogeneous Nucleation

Nicolas Garcia Garcia[a] and Jose M. Soler Torroja[a]
Department of Aeronautics and Astronautics, Massachusetts Institute of Technology, Cambridge, Massachusetts 02139
(Received 20 October 1980)

Monte Carlo calculations of the free energy of argon clusters are presented. The resulting homogeneous nulceation rates are in reasonable agreement with the experimental data over a wide range of pressures (10^{-4} atm$<p<2\times10^{-1}$ atm) and temperatures (25°K $<T<$ 60°K) at the onset of condensation.

PACS numbers: 64.70.Fx, 61.20.Ja, 61.25.Bi

Precise experiments on argon condensation by isothermal, steady-state, homogeneous nucleation from a supersaturated vapor have been carried out by Stein[1] and Wu, Wegener, and Stein.[2] Argon seems to be one of the easier vapors to study theoretically because of its simple Lennard-Jones interaction potential. Nevertheless up to now no calculation has given agreement with experiments over a wide range of temperatures (25 °K $<T<$ 60 °K) and pressures (10^{-4} atm $<p<2\times10^{-1}$ atm) at the onset of condensation. Recently Hoare, Pal, and Wegener[3] have calculated free energies and nucleation rates for argon microclusters using an icosahedron-based packing and the harmonic approximation. It is known by comparisons with "exact" Monte Carlo calculations[4,5] that the harmonic approximation underestimates the free energies of cluster formation because it does not include anharmonicity or the entropy due to shape change. But it should be said that the point of view in Ref. 3 is a step forward in treating this problem by calculating the free energies.

In this work we report on a Monte Carlo calculation of free energies of formation of argon microclusters. The intermolecular potential is a Lennard-Jones potential. The cluster sizes go from two to thirty-seven molecules and the reduced temperature $T^*=kT/\epsilon$ (where ϵ is the Lennard-Jones well depth) varies between 0.2 and 0.7 with intervals $\Delta T^*=0.05$.

Knowing the free energies it is possible to obtain nucleation rates and to compare them to experimentally obtained rates. Our calculated rates prove to be in good agreement with the reported data.[1,2]

We assume that cluster growth takes place by monomer addition according to the reaction:

$$A_1+A_{n-1}\rightleftarrows A_n. \tag{1}$$

If we assume a steady-state solution, the nucleation rate J may be calculated from the equilibrium concentrations C_n of the n clusters. It reads[3,4,6]

$$J=\alpha\beta/\sum_{n=1}^{N}(O_nC_n)^{-1}, \tag{2}$$

where N is the maximum cluster size after which the nucleation rate is unaffected, α is the sticking coefficient and is taken to be equal to unity, β is the rate at which atoms of mass m at the state (p, T) impinge on a unit area, and O_n is the surface area of a cluster of size n. The quan-

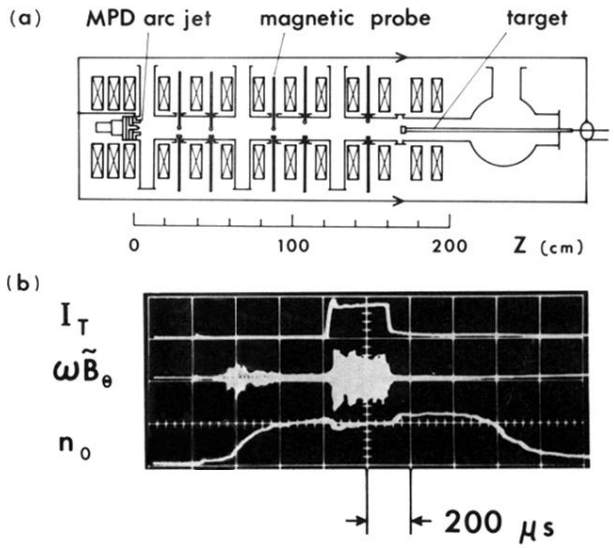

FIG. 1. (a) Experimental apparatus. Loops of return current are also shown. (b) Time evolutions of target current, azimuthal magnetic field fluctuation, and density.